

# CFD Investigation of Industrial Gas-Liquid Preneutralizer Based on a Bioreactor Benchmark for Spargers Optimization

Safae Elmisaoui<sup>a,b,\*</sup>, Sanae Elmisaoui<sup>a,c</sup>, Saad Benjelloun<sup>a</sup>, Lhachmi Khamar<sup>d</sup>, Mohamed Khamar<sup>b</sup>

<sup>a</sup> Mohammed VI Polytechnic University (UM6P), MSDA Group, Morocco

<sup>b</sup> Mohammed V University, LGCE, Rabat, Morocco

<sup>c</sup> Laboratoire Réactions et Génie des Procédés, CNRS-ENSIC, Université de Lorraine, Nancy, France

<sup>d</sup> Sultan Moulay Slimane University, LIPIM, ENSA-Khouribga, Morocco

safae.elmisaoui@um6p.ma

In this paper, a benchmark study between chemical and biochemical reactors is carried out using Computational Fluid Dynamics (CFD) approach. The main motivation is to develop an optimized design of a stirred sparged gas liquid reactor for preneutralisation of phosphoric acid. A CFD multiphase model is tailored under ANSYS Fluent 2020 R1, to simulate the industrial preneutralizer. A new gas sparger is designed based on fermentation bioreactors ring spargers for axial gas dispersion. The Euler-Euler multiphase reacting flow model is used within the preneutralizer to examine the impact of the spargers type on the hydrodynamics, species transport phenomena, and mass transfer between the different phases. K-Epsilon turbulence model is adopted to integrate the turbulence due to the Pitch Blade Turbine (PBT) agitator, and Multiple Reference Frame (MRF) approach allows to handle efficiently the rotational movement of the agitator. The simulations show that ring spargers enhance mass transfer by ensuring a high level of gas phase holdup with the axial dispersion compared to the pipe spargers. The numerical results revealed that gas-liquid flow hydrodynamics is extremely sensitive to the sparger design. The proposed new preneutralizer design is promising to increase the preneutralisation yield and allows to avoid several monitoring challenges.

## 1. Introduction

In chemical and biochemical industries, many operation units involve gas-liquid multiphase flows. Stirred tank reactors have been used frequently in many chemical processes (Elmisaoui et al., 2021), these reactors represent the masterpiece affecting the product quality (Li et al., 2017). In phosphate fertilizers manufacturing processes, a phosphoric acid preneutralizer with ammonia injection produces a slurry to be converted into granules by feeding the drum ammoniator-granulator (Henry et al., 2013). The preneutralizer (PRN) reactor is a non-standard stirred tank reactor, equipped by a pitched blades turbine that promotes mass and heat transfer. It also reduces foaming and improve ammonia absorption. The “preneutralization” chemical reaction consists on the ammonia gas reaction with crude phosphoric acid (ACP) (Liquid) to produce some nitrogen containing compounds (slurry). Two principal compounds of major importance forming in this reaction are Di Ammonium Phosphate (DAP) and Mono Ammonium Phosphate (MAP). The chemical equation showing the principal reaction is listed below:



This reaction occurs immediately when  $\text{NH}_3$  and  $\text{H}_3\text{PO}_4$  are mixed. Depending to the mole ratio between these reactants, the intermediate production of MAP happens, then the excess ammonia converts MAP ( $(\text{NH}_4)\text{H}_2\text{PO}_4$ ) to DAP ( $(\text{NH}_4)_2\text{HPO}_4$ ).

The performance of the PRN depends mainly on the operating parameters and geometrical characteristics (Elmisaoui et al., 2020). The type of agitator, the design of the injectors and their positions are key parameters to improve the hydrodynamics, and thus better control the transport phenomena between the chemical species present in the system. The current geometrical conditions of the ammonia pipe injectors generate losses of a high rate of gaseous ammonia. The hydrodynamics in the area near to the slurry outlet, and the power of the flow absorbed by the pump to the granulator, allows considerable amount of ammonia to leave the reactor just after injection. This is especially true for feeds from radial spargers near to the slurry outlet, which requires to put them in off mode in the current process and operate the PRN with only six injectors, which decreases considerably the efficiency of the preneutralizer. The maturity of gas liquid chemical reactors in biotechnology, especially in oxidation bioreactors and fermenters, proved that gas sparger design governs the flow hydrodynamics in gas liquid sparged stirred reactor (Birch et al., 1997). It has been demonstrated that gas sparger design, dimensions and location have significant effect on the gas dispersion and the flow behavior. Many designs are used (conical sparger, jet distributor, ring sparger, tubular sparger, etc.) and the performance of each type depends on system characteristics (Li et al., 2021).

Hence, the main objective of this study is to use CFD modelling to investigate the effect of changing the radial classical ammonia sparger by a new design based on ring sparger and to quantify the PRN performance in terms of mixing and mass transfer.

## 2. CFD modelling strategy

The numerical model is based on the Eulerian Multifluid approach, and has been carried out using the commercial CFD software ANSYS Fluent 2020 R1. Details of the model will be described in the following subsections.

### Computational domain and geometry design

The PRN geometrical model is based on the industrial scale dimensions, as shown in Figure 1, the working volume of that reactor is  $47 \text{ m}^3$  to ensure a throughput around  $120 \text{ m}^3/\text{h}$ . It is equipped by a PBT agitator, with four impellers slanted with  $45^\circ$  from the horizontal plane. The impeller diameter is 2.5 m and is placed at a height of 0.9 m from the bottom. The impeller motion was modelled by the inner-outer model, based on the MRF approach. The ACP liquid is injected from the top, and the ammonia spargers are implemented near to the bottom. Figure 1. (a) and (b) represents the used geometries in this work, with the original and the new proposed spargers. In the design of the new sparger, the diameter of the ring is determined based on the distance between the original radial injectors outlets and the tank wall. This ensures the same flow throughput by each injector similarly to the original feeds. The system boundary conditions and physical settings are based on the operating conditions at the industrial scale.

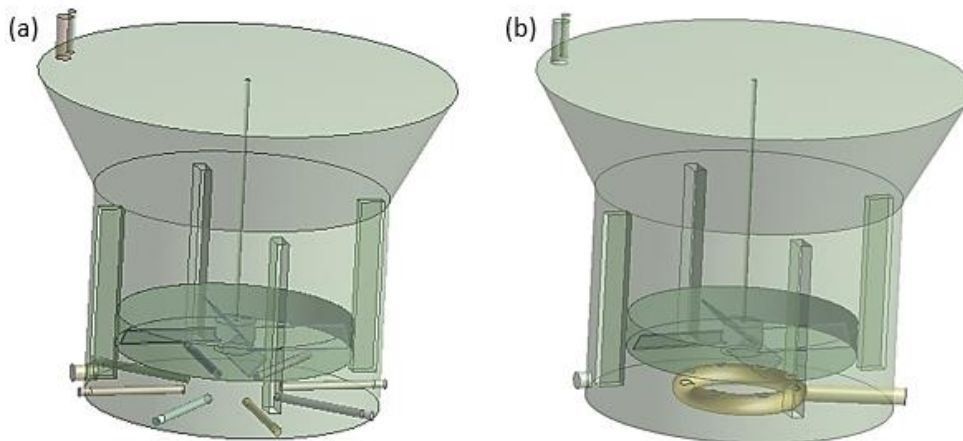


Figure 1: The PRN geometry with gas spargers modification, (a) original, (b) new sparger

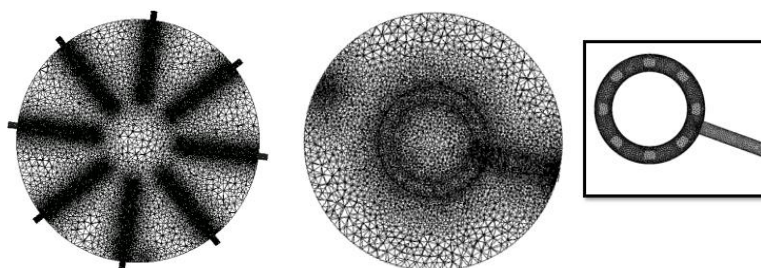
Table 1. reports the physical parameters used for this study

*Table 1: Parameters of the study*

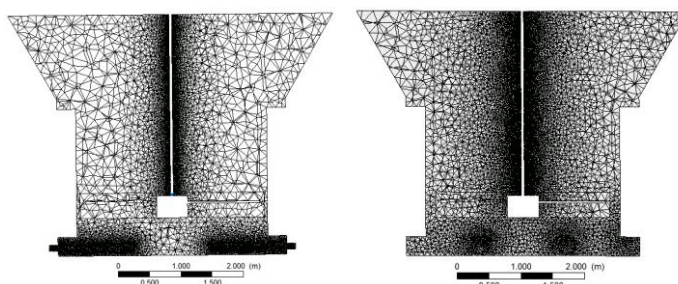
Simulation parameters	Symbol	Value	Unit
Height of the reactor	H	7.3	m
Width of the reactor	W	3.65	m
NH <sub>3</sub> injection area diameter	d	0.104	m
NH <sub>3</sub> gas density	$\rho_g$	1.215	kg/m <sup>3</sup>
NH <sub>3</sub> dynamic viscosity	$\mu_g$	1.8 e <sup>-5</sup>	Pa.s
ACP liquid density	$\rho_l$	2650	kg/m <sup>3</sup>
ACP liquid viscosity	$\mu_l$	0.021	Pa.s
Operating temperature	T	80	°C

### Domain meshing

The ANSYS meshing tool is used to generate an unstructured grid composed by tetrahedral elements. Mesh quality has been evaluated and mesh convergence analysis has been conducted to use the optimal grid in terms of computational time and accurate results. Figure 2. a and b show cross-sectional and frontal views of these meshes.



*Radial cross section at the level of middle spargers plane, with zoom in the new sparger (1076818 cells)*



*Frontal view of the mesh domain at the middle of the PRN (1162588 cells)*

*Figure 2: Overview of the computational domain mesh*

### 2.3. Flow model, governing equations and species transport

In this work the Euler-Euler multi-fluid model is adopted where gas and liquid phases are all treated as interpenetrating continua, in the computational domain. The Euler-Euler (EE) approach is suitable for modelling such two fluid flow in a stirred reacting tank with the sparged gas bubbles. Compared to the Euler-Lagrange (EL), it is more efficient in terms of computing time and has acceptable accuracy for the desired applications. The motion of each phase is governed by respective mass and momentum conservation equations (Maluta et al., 2021). The mass conservation equation is written as follows:

$$\frac{\partial(\rho_\varphi \alpha_\varphi)}{\partial t} + \nabla \cdot (\rho_\varphi \alpha_\varphi \mathbf{u}_\varphi) = S_m \quad (2)$$

The equation for conservation of momentum in the  $i^{\text{th}}$  direction is defined by:

$$\frac{\partial(\rho_\varphi \alpha_\varphi)}{\partial t} + \nabla \cdot (\rho_\varphi \alpha_\varphi \mathbf{u}_\varphi \mathbf{u}_\varphi) = -\alpha_\varphi \nabla p + \nabla \cdot (\mu_{\varphi,eff} \alpha_\varphi (\nabla \mathbf{u}_\varphi + (\nabla \mathbf{u}_\varphi)^T)) + \rho_\varphi \alpha_\varphi \mathbf{g} + \mathbf{F}_\varphi \quad (3)$$

Where  $\rho_\varphi$ ,  $\alpha_\varphi$ , and  $\mathbf{u}_\varphi$  are the density, volume fraction, and mean velocity vector of phase  $\varphi$ , respectively, where the subscript  $\varphi$  refers to the liquid (l) or gas (g) phase. The source term  $S_m$  models the mass added through phase changes.

To solve the conservation equations for the chemical species in multiphase flows, within each phase  $q$ , we need to predict the local mass fraction,  $Y_i^q$ , through the solution of a Convection-Diffusion equation for the  $i^{\text{th}}$  species. The chemical species conservation equation, when applied to a multiphase flow can be represented in the following form:

$$\frac{\partial}{\partial t} (\rho^q \alpha^q Y_i^q) + \nabla \cdot (\rho^q \alpha^q \bar{\mathbf{v}}^q Y_i^q) = -\nabla \cdot \alpha^q \mathbf{J}_i^q + \alpha^q R_i^q + \alpha^q S_i^q + \sum_{p=1}^n (\dot{m}_{p^i q^j} - \dot{m}_{q^i p^j}) + \mathcal{R} \quad (4)$$

where  $R_i^q$  is the net rate of production of homogeneous species  $i$  by chemical reaction for phase  $q$ ,  $\dot{m}_{p^i q^j}$  is the mass transfer source between species  $i$  and  $j$  from phase  $q$  to  $p$  and  $\mathcal{R}$  is the heterogeneous reaction rate. The reaction rates are scaled by the volume fraction of the phase in the cell. For our case we supposed that the system is non-reacting. The energy equation is also considered to represent heat exchanges.

#### 2.4. Turbulence model

Reynolds Averaged Navier Stokes Equations (RANS) provide an efficient model for turbulence in industrial scale systems. In this study, the RNG  $k$ - $\epsilon$  model is used and two additional equations balancing turbulent kinetic energy  $k$  and rate of energy dissipation  $\epsilon$  for each phase are coupled to Navier Stokes equations.

#### 2.5. Numerical model

The solver setting included phase coupled algorithm for pressure – velocity coupling and a finite volume method. The special discretization was set to QUICK for the volume fraction, combined with a second order scheme for the turbulence equations and the second-order backward Euler scheme for the transient terms. The underrelaxation factors of the numerical scheme were set initially to 0.3 for pressure, 0.4 for momentum and 0.2 for the species volume fraction. The convergence criterion was set to  $1 \times 10^{-4}$  for scalars, chemical species volume fractions, and velocities. For both cases simulations were run for a period of 50 s, and a reasonable convergence was achieved with residuals less than  $10e-5$  for all the equations of the system.

### 3. Results

#### 3.1. Flow field hydrodynamics

CFD model results show that the hydrodynamics within the preneutralizer depend directly on the spargers type. Figure 3 represents the ammonia gas distribution at the radial plane splitting the spargers from the middle, after 30s of simulation time, allowing the gas phase to attain the spargers outlets and to mix with the ACP liquid. In Figure 3. (a) the gas injected by the pipe sparger near to the slurry is subject to the aspiration form the pump in this boundary, which represents the same phenomenon observed in the industrial facility.

A proportion of 80% of the ammonia gas injected is well dispersed overall the PRN with the new sparger design, otherwise in the zone with the principal ammonia inlet, the injected gas phase is imported to the other zone, by mixing. Also, the shape of this ammonia distributor represents an obstacle to inhomogeneous flow which impacts the hydrodynamics and transfer mechanisms further. Changes about the position of this latter are required. On other hand, the combination of a PBT and ring spargers allows a good axial dispersion of the injected ammonia Figure 3. (d), compares to the dispersion observed with a pipe sparger Figure 3. (c). The gas attains the turbulent zone very fast that for the pipe injector case, which will increase the reaction rate and decreases the required time to achieve system homogeneity.

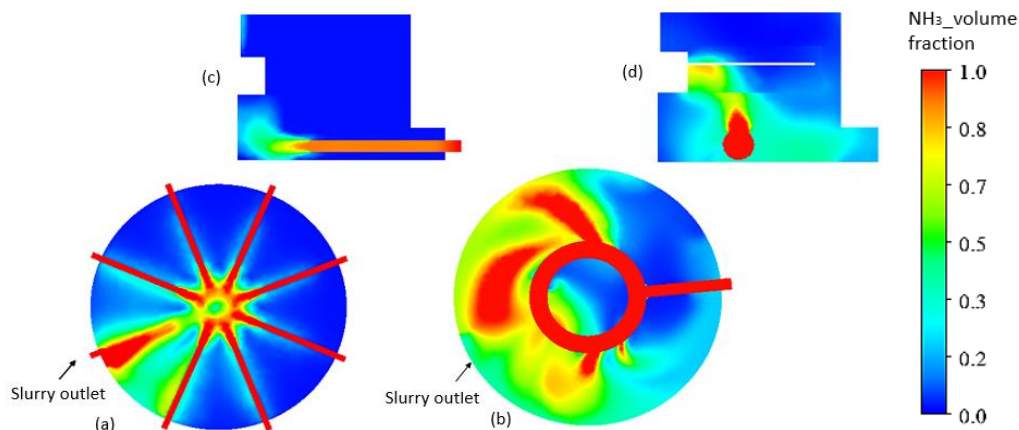


Figure 3: Ammonia gas distribution in the radial plane splitting spargers ( $X=0.3m$ ,  $t=40s$ ), respectively for (a) pipe and (b) ring spargers, with a zoom on the axial distribution of ammonia in injection zone (c) pipe, (d) ring spargers.

### 3.2. Gas holdup distribution and mass transfer

When the ammonia gas is sparged in the PRN, it rises upwards due to the buoyancy force associated with this phase. It then diffuses or escapes in the liquid phase. We defined six probe points to follow the gas holdup within the PRN. It was observed that, for P1, P2, P3, P4 and P5 the ammonia gas is detected for both designs, and the gas dispersion decreases when rising in the vessel. At the radial plane containing P6 point ( $z = 4.5$  m), the  $NH_3$  phase is not detected with geometry representing pipe spargers, but it attains some specific zones with the new proposed geometry, which reflects that only some spargers are effective (Figure 4 (b)). Previous experimental study validated our results (Rewatkar et al., 1993). Hence, the change of the sparger type to the ring one implicates new operating conditions. For instance; the gas flow rate or geometrical characteristics (sparger diameter, location, ring diameter, etc.) are manipulated for a good hydrodynamics.

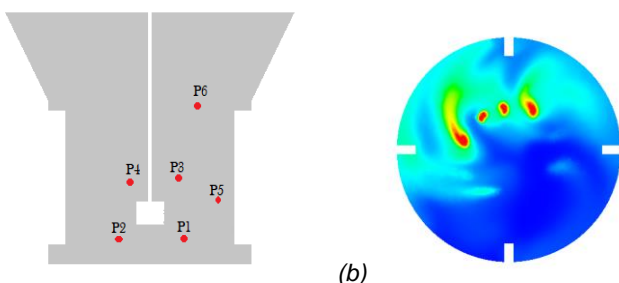


Figure 4: (a) frontal view of the PRN with probes, (b) upper plane (P6)

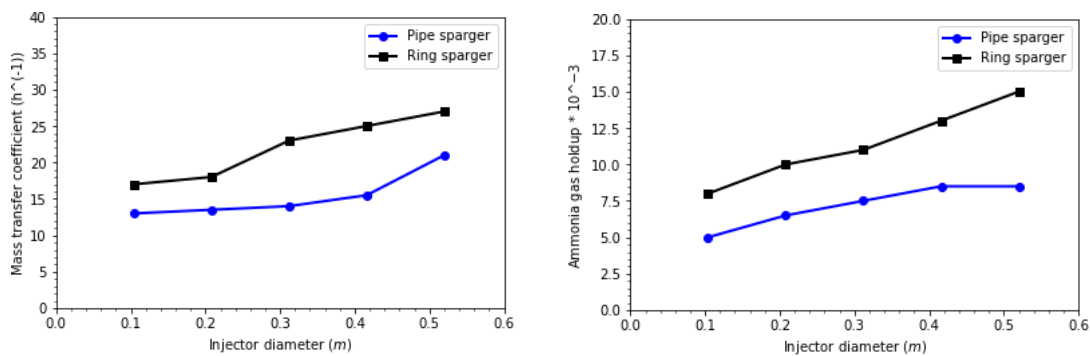


Figure 5: Comparison of mass transfer coefficient (a) and ammonia gas holdup (b) for pipe and ring spargers for different injector diameters

Figure 5 shows the comparison of mass transfer coefficient and ammonia gas holdup for five injector diameters in the range of 0.104 m – 0.6 m in both cases, with fixed bubbles diameter ( $d_b = 0.5$  mm) using mean Sauter diameter for a uniform bubbles family. The rotational speed is defined by its operational value (68 rpm). The ammonia gas holdup increases with the diameter of injectors and better values are achieved for bigger diameter until some point where the use of bigger spargers led to a cavitation zone under the agitator. With the depression caused in the same place, the gas has difficulty to access the impeller region. This effect is more and more pronounced in the case of ring spargers when the size of injectors exceeds 0.3 m. From other point of view, the mass transfer coefficient is enhanced by increasing diameters. Figure 5 (b) shows higher values with the ring sparger compared to the pipe sparger over the different diameters, but the flow pattern in the two biggest one (0.416 m – 0.52 m) of this injector is quite different from those generated by the other three spargers. This is due to the stirred sparged gas liquid reactors design, where the sparging diameter and the vessel diameter should ensure a ratio of  $d_{sp}/D = 0.8$  as recommended by McFarlane (McFarlane et al., 1995).

#### 4. Conclusions

A three-dimensional Eulerian-Eulerian gas- liquid CFD model is developed using ANSYS 2020 R1, allowing to evaluate the effect of sparger design on the hydrodynamics within the preneutralizer. k-Epsilon turbulence model and MRF approach were used. The mass transfer, gas holdup and dispersion are numerically investigated.

A new ring sparger is designed inspired from bioreactors, and its effect is investigated on the preneutralizer performance, especially for mass transfer and gas holdup. The model provides good agreement with previous literature studies, and confirms our design recommendations. The new designed sparger proves its efficiency in enhancing the ammonia dispersion within the preneutralizer. The mass transfer coefficient and gas holdup sensitivity to the sparger diameter was examined, and the actual diameter increasing leads to enhancing these key parameters, up to the ratio  $d_{sp}/D = 0.8$ . Further work is ongoing to improve the preneutralization manufacturing by experimenting the proposed sparger design.

#### Nomenclature

ACP – Phosphoric Acid	MRF – multiple reference frame
CFD – Computational fluid dynamics	PTB – pitch blade turbine
DAP – Di Ammonium Phosphate	RNG – Renormalization Group
PRN – Preneutralizer	RANS – Reynolds Averaged Navier Stokes

#### Acknowledgments

This work was financially supported by Mohammed VI Polytechnic University and OCP Group. UM6P and OCP (S.A) are hereby acknowledged.

#### References

- Birch, D. and Ahmed, N., 1997. The influence of sparger design and location on gas dispersion in stirred vessels. *Chemical Engineering Research and Design*, 75(5), pp.487-496.
- Elmisaoui, S., Khamar, L., Benjelloun, S., Khamar, M. and Ghidaglia, J.M., 2020. Modeling and Study of Hydrodynamic flow within the Preneutralizer Reactor using CFD Approach. In *Computer Aided Chemical Engineering* (Vol. 48, pp. 103-108). Elsevier.
- Elmisaoui, S., Latifi, A.M., Khamar, L. and Salouhi, M., 2021. Shrinking Core Approach in the Modelling and Simulation of Phosphate Ore Acidulation. *Chemical Engineering Transactions*, 86, pp.871-876.
- Henry, J. 2013. Operating manual of Di Ammonium Phosphate process, (internal document). Times Lit. Suppl., no. 5911, p. 29,
- Li, L., Zhao, Y., Lian, W., Han, C., Zhang, Q. and Huang, W., 2021. Review on the Effect of Gas Distributor on Flow Behavior and Reaction Performance of the Bubble/Slurry Reactors. *Industrial & Engineering Chemistry Research*, 60(30), pp.10835-10853.
- Li, X., Guan, X., Zhou, R., Yang, N. and Liu, M., 2017. CFD simulation of gas dispersion in a stirred tank of dual Rushton turbines. *International Journal of Chemical Reactor Engineering*, 15(4).
- Maluta, F., Paglianti, A. and Montante, G., 2021. CFD Prediction of Gas-filled Cavity Structures in Aerated Vessels Stirred with Multiple Rushton Turbines. *Chemical Engineering Transactions*, 86, pp.1135-1140.
- McFarlane, C.M., Zhao, X.M. and Nienow, A.W., 1995. Studies of high solidity ratio hydrofoil impellers for aerated bioreactors. 2. Air-water studies. *Biotechnology progress*, 11(6), pp.608-618.
- Rewatkar, V.B., Deshpande, A.J., Pandit, A.B. and Joshi, J.B., 1993. Gas hold-up behavior of mechanically agitated gas-liquid reactors using pitched blade downflow turbines. *The Canadian Journal of Chemical Engineering*, 71(2), pp.226-237.